TITLE PAGE

The pre-supplementary motor area achieves inhibitory control by modulating response thresholds

Noham Wolpe[1,2,3], Frank H. Hezemans[4,5], Charlotte L. Rae[6.7], Jiaxiang Zhang[8], James B. Rowe[4,5]

[1]Department of Physical Therapy, The Stanley Steyer School of Health Professions, Faculty of Medicine, Tel Aviv University, Tel Aviv 6997801, Israel.

[2]Sagol School of Neuroscience, Tel Aviv University, Tel Aviv 6997801, Israel

[3]Department of Psychiatry, University of Cambridge, Cambridge CB2 0SZ, UK.

[4]MRC Cognition and Brain Sciences Unit, University of Cambridge, Cambridge CB2 7EF, UK.

[5]Department of Clinical Neurosciences, University of Cambridge, Cambridge CB2 0QQ, UK.

[6]School of Psychology, University of Sussex, Brighton BN1 9RH, UK.

[7]Sackler Centre for Consciousness Science, University of Sussex, Brighton BN1 9RH, UK.

[8]Cardiff University Brain Research Imaging Centre, Cardiff University, Cardiff CF24 4HQ, UK.

Running title: pre-SMA modulates inhibition thresholds

Correspondence should be addressed to:

Dr Noham Wolpe

E-mail: nwolpe@tau.ac.il

Faculty of Medicine

The Stanley Steyer School of Health ProfessionsTel Aviv University P.O. Box 39040,

Tel Aviv 6997801

Telephone: +972 (0) 6405460

ABSTRACT

The pre-supplementary motor area (pre-SMA) is central for the initiation and inhibition of voluntary action. For the execution of action, the pre-SMA optimises the decision of which action to choose by adjusting the thresholds for the required evidence for each choice. However, it remains unclear how the pre-SMA contributes to action inhibition. Here, we use computational modelling of a stop/no-go task, performed by an adult with a focal lesion in the pre-SMA, and 52 age-matched controls. We show that the patient required more time to successfully inhibit an action (longer stop-signal reaction time) but was faster in terms of go reaction times. Computational modelling revealed that the patient's failure to stop was explained by a significantly lower response threshold for initiating an action, as compared to controls, suggesting that the patient needed less evidence before committing to an action. A similarly specific impairment was also observed for the decision of which action to choose. Together, our results suggest that dynamic threshold modulation may be a general mechanism by which the pre-SMA exerts its control over voluntary action.

INTRODUCTION

The pre-supplementary motor area (pre-SMA) is a cardinal site of voluntary action: electrical stimulation here famously elicits an urge to move (Fried et al., 1991), while fMRI meta-analyses show pre-SMA activity across multiple decisions required for voluntary actions, including which action perform; when to perform an action; and whether to perform it in the first place (Brass & Haggard, 2008; Zapparoli et al., 2017). In the decision of whether to perform an action or to withhold it, the pre-SMA has a critical role in action inhibition. It is consistently identified in fMRI studies of motor inhibition tasks in young and old adults, such as the stop signal task that requires action cancellation, and the go/no-go task that requires action prevention (Rae et al., 2014, 2015; Swick et al., 2011). Transcranial magnetic stimulation to the pre-SMA and focal brain lesion in this area both impair stopping, by lengthening the stop signal reaction time (SSRT) required to successfully cancel an action (Chen et al., 2009; Floden & Stuss, 2006). Lastly, altered pre-SMA activity is associated with impulsivity due to neuropsychiatric (Dickstein et al., 2006) and neurodegenerative (Passamonti et al., 2018) conditions and results in inappropriately afforded, unwanted actions (Wolpe et al., 2014).

Although the critical role for the pre-SMA in stopping is widely established, the latent cognitive mechanisms by which it exerts its effect is not. Performance on the stop signal task is commonly conceptualised as a ‘two-horse race’ between ‘go’ and ‘stop’ processes, such that whichever is completed first determines the outcome (with go leading to action execution, and stop leading to action cancellation) (Logan & Cowan,

1984). Several cognitive processes influence whether the go or stop process completes the race first, such as rate of information processing, motor preparation, speed-accuracy trade-offs, response bias, and trigger failures. However, it is not clear which of these processes relate to the pre-SMA (Sebastian et al., 2018).

One way to operationalise the specific processes performed by the pre-SMA in stopping is by adopting models used in decision making research. A model-based approach commonly used to identify the latent mechanisms underlying decision making is sequential sampling models, such as the drift-diffusion model (DDM) (Limongi et al., 2018; Ratcliff & Van Dongen, 2011). Such a model represents the processes of accumulating evidence for making the decision of which option to choose (e.g., whether to act or to withhold an action), until evidence reaches a certain threshold. The rate of evidence accumulation and threshold are typically parametrised in these models, as well as other 'non-decision' time. In decision making paradigms, such as perceptual decision making with speed-accuracy trade-offs, several studies have shown that the pre-SMA supports the selection of action by adjusting the thresholds for the amount of evidence required for deciding which action to choose (Cavanagh et al., 2011; Mulder et al., 2014; Tosun et al., 2017). For example, trial-to-trial changes in pre-SMA fMRI activity correlate with trial-to-trial changes in decision threshold (van Maanen et al., 2011). However, it is not currently clear whether the pre-SMA exerts inhibitory control by similarly modulating response thresholds for whether to act.

Here, we tested this hypothesis by using computational modelling in a patient with a precise focal lesion in the pre-SMA. While fMRI studies correlating model parameters with brain activity have numerous advantages, testing a patient with a focal lesion limited to the pre-SMA would enable to test for a causal role of pre-SMA in stopping. We capitalised on recent developments in hierarchical Bayesian model estimation in order to compare the single patient case to controls, by estimating each model's posterior distribution and comparing these distributions between patient and controls. Specifically, we compared the model-based estimated SSRTs (Matzke et al., 2013) and response thresholds (Wiecki et al., 2013). We predicted that pre-SMA lesion would lead to an impairment in normal inhibition, which would be reflected in abnormally long SSRT, and which will be critically explained by low threshold for initiating an action.

METHODS

Participants

A 74-year-old man with a focal brain lesion in the pre-SMA (Fig. 1) was recruited from the Cambridge Cognitive Neurosciences Research Panel (CCNRP), at the Medical Research Council Cognition and Brain Sciences Unit. Ten years prior to the experiment, he was diagnosed with deep vein thrombosis and commenced on warfarin. Shortly after anticoagulation, he suffered from a small subarachnoid haemorrhage which was revealed by brain imaging, together with a 6 cm right-sided meningioma. He underwent a successful surgical resection. The patient was neurologically asymptomatic before the bleed, and had made an excellent recovery to normal by 6 month and 18 month post-operative clinical reviews. No sensorimotor or cognitive impairments were reported, and he was described in post-operative notes as functionally normal. At the time of testing, he had no symptoms and there was no symptomatic motor functional impairment. Mini-mental state examination score was 28/30 (Folstein et al., 1975).

Normative control data were taken from the third stage ("CC280") of the Cambridge Centre for Ageing and Neuroscience (Shafto et al., 2014), in which participants performed the same stop signal task (Tsvetanov et al., 2018). Data from all participants aged 60 and older were used, which after the exclusion of four participants who had no button press data, made up a total of 52 healthy controls (26 females; M = 74 years, SD = 8 years, range = 60-92 years; MMSE mean = 29, SD = 1). The study was approved by the Cambridgeshire 2 (now East of England—Cambridge Central)

Research Ethics Committee. All participants provided a written informed consent prior to the study.

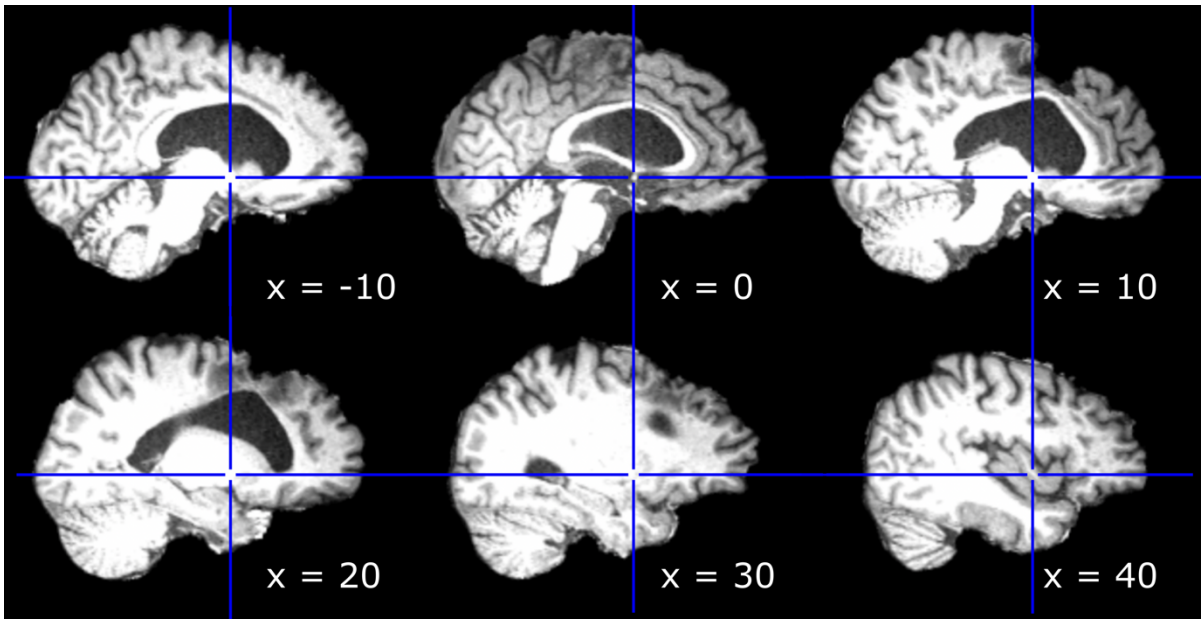

Figure 1. Patient structural T1 MRI scan. Intracranial volume was extracted using FSL Brain Extraction Tool (Smith, 2002). For orientation, the origin [0, 0, 0] (blue crosshair) was set to the Anterior Commissure (AC) and the scan was aligned to the Anterior Commissure – Posterior Commissure (AC-PC) line. The lesion was focal to the pre-supplementary motor area with minimal extension to the more posterior supplementary-motor area proper (y coordinates smaller than 0). X coordinates shown for each slice.

Stop signal task

The control group and the patient performed a stop signal task (Fig. 2; Logan et al., 1984). The task included pseudo-randomly interleaved action ('Go'), action cancellation ('Stop') and action prevention ('No-Go') trials. All trial types were preceded by a fixation cross for 500 ms. In Go trials, a left or right black arrow was displayed for 1000 ms, requiring participants to respond by pressing the correct left or

right button with their dominant hand (index and middle fingers). In Stop trials, the right or left black arrow was initially displayed, but after a delay (the stop signal delay; SSD), the arrow changed its colour to red and a pure tone was played (1000 Hz), requiring participants to cancel their action and withhold from pressing the button. The length of the SSD was initially randomly set to either 250 ms or 300 ms, and then determined for each trial by a staircase algorithm, so as to allow successful inhibition in about 50% of the stop trials. To reduce the tendency for participants to strategically slow their responses on stop signal tasks, three parallel algorithms were used (Rae et al., 2014). In No-Go trials, the SSD was set to 0 ms, such that a red left or right arrow was displayed for 1000 ms and the simultaneous sound was played from the beginning of the trial. No-Go trials were included as attentional catch control trials, as No-Go uses different mechanisms to action cancellation (Swick et al., 2011). The patient performed 360 trials in total, with 270 Go trials, 60 Stop trials and 30 No-Go trials, over two runs with a short break in between. Controls performed a longer version of the task in the fMRI scanner, which included 480 trials in total, with 360 Go trials, 80 Stop trials and 40 No-Go trials, again run over two runs with a short break in between. Importantly, the proportions of each trial type were identical in the patient and controls.

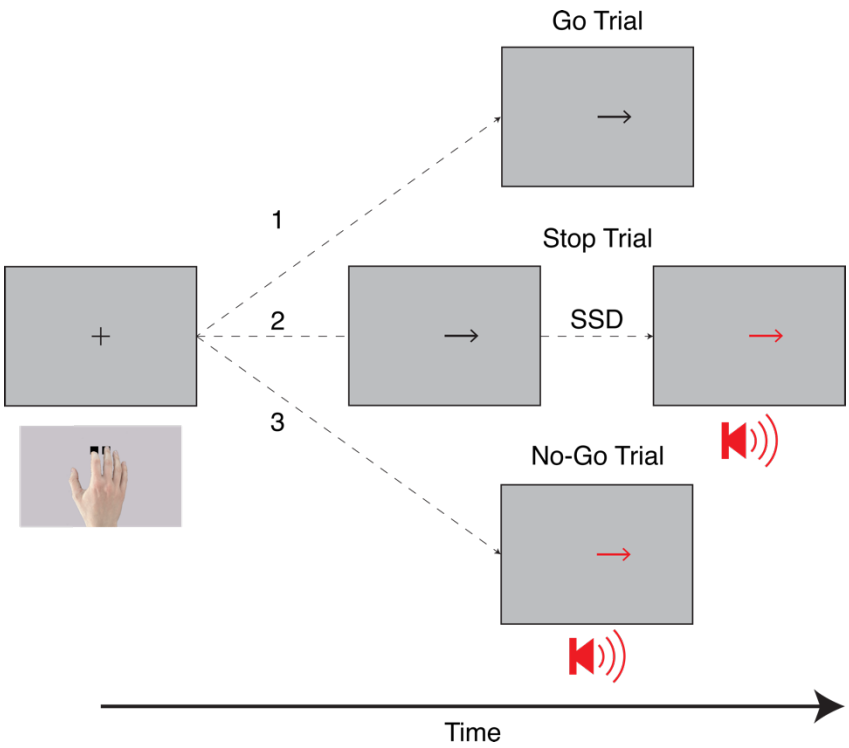

Figure 2. **Illustration of the Stop No-Go Task.** Each trial in the Stop No-Go task began with a fixation cross, followed by the display of an arrow stimulus. The task included three trial types (indicated by the numbers 1-3): 1) Go trial, in which participants were asked to press a button with their index or middle finger to indicate whether the arrow was pointing right or left. 2) Stop trial, which the arrow was similarly displayed at first, but following a varying stop signal delay (SSD), the arrow changed its colour from black to red, and a tone was played, requiring participants to withhold the button press. 3) No-Go trial, in which SSD was set to 0 ms, and hence the arrow was displayed in red, and a tone was played from the start.

Estimation of SSRT

As a descriptive measure of response inhibition, we estimated the stop signal reaction time (SSRT) using a parametric model of the stop signal task (Matzke et al., 2013, 2019). This model assumes a race between three independent processes: one corresponding to the Stop process, and two corresponding to Go processes that match or do not match the Go stimulus. Successful inhibition on a Stop trial occurs when the

Stop process finishes before both Go processes. For a given Go trial, a correct response occurs when the matching Go process finishes before the mismatching Go process. The model assumes that the finish times of these processes follow an ex-Gaussian distribution, which is a positively skewed unimodal distribution that is commonly used to describe reaction time data (Heathcote et al., 1991). For each of the three processes, the model estimates the three parameters of the ex-Gaussian distribution: The mean μ and standard deviation σ of the Gaussian component, and the mean (i.e., inverse rate) τ of the exponential component. The model additionally estimates two parameters that represent the probability that the Stop and Go processes failed to start, referred to as “trigger failure” and “go failure”, respectively (Matzke et al., 2019). Such attentional failures are common in healthy participants (Matzke, Love, et al., 2017; Skippen et al., 2019) and in clinical cohorts (Matzke, Hughes, et al., 2017; Weigard et al., 2019), and, if not modelled, can severely bias estimates of SSRT (Band et al., 2003; Matzke et al., 2019).

SSRT was the principal parameter of interest and was computed as the mean of the ex-Gaussian finish time distribution of the Stop process, which is given by $\mu_{stop} + \tau_{stop}$. We additionally computed go RT as the mean of the matching Go process ($\mu_{go\text{-}match} + \tau_{go\text{-}match}$). Note that the ex-Gaussian is a purely descriptive model of the Stop process finish time distribution, and its parameters (μ_{stop}, σ_{stop}, and τ_{stop}) are not necessarily equivalent to parameters of a drift-diffusion process (Matzke et al., 2020; Matzke & Wagenmakers, 2009).

Drift diffusion model of response times

We used drift diffusion models to decompose the processes underlying the decision to act or to withhold an action. Considering the current technical challenges of directly estimating evidence accumulation parameters of the Stop process (Matzke et al., 2020), we opted for a one-choice RT model (Limongi et al., 2018; Ratcliff & Van Dongen, 2011). On this approach, the decision to respond and press a button can be conceptualised as a drift process that accumulates evidence over time as to whether the current trial is a Go or a Stop trial. Evidence is accumulated until a certain boundary is crossed, when the participant commits to the decision to press the button. Such a basic 'drift-diffusion model' (Ratcliff & McKoon, 2008) includes three free parameters, namely: the decision threshold ('a') which is the distance between boundaries; the average rate in which the drift process approaches the boundaries ('v'); and the non-decision time normally described as the sum of stimulus encoding and action execution times ('t'). We fit this model to RTs of responses in the stop signal task. As our main interest was in the mechanism underlying failure to inhibit with a pre-SMA lesion, our principal model focused on the subset of Stop trials in which participants failed to inhibit their response (commission errors). In a complementary analysis, we examined the latent cognitive variables of the decision of which action to choose. To this end, we fit a two-choice DDM to all Go trials with a response (i.e., excluding omission errors), using the standard model of accuracy-coded responses (Wiecki et al., 2013). For both DDMs, we also fit a model that estimated inter-trial variability in non-decision time 'st', as previously discussed (Ratcliff & Tuerlinckx, 2002). The parameters reported in the main text were from the model with the significantly lowest

deviance information criterion (Wiecki et al., 2013) (Supplementary Materials; Figures S4-S5).

Bayesian hierarchical model fitting

In order to generate a robust estimation of the posterior distributions of each model's parameters, we used a Bayesian hierarchical model fitting procedure to fit the data. For the control group, model fitting was performed hierarchically, such that parameters for a given participant were sampled from corresponding group-level normal distributions. This hierarchical approach allows for a reliable group-level inference of parameter distributions, as it takes into account the data from all participants simultaneously, while explicitly modelling individual differences (Daw, 2011; Farrell & Lewandowsky, 2018; Gelman et al., 2014). The patient data were fit separately so as to provide a separate posterior distribution for statistical comparison (see below). We generally assigned relatively broad ("weakly informative") prior distributions on the model parameters; a full list of priors is provided in the Supplementary Materials (Table S1). Markov Chain Monte Carlo (MCMC) sampling methods were used to estimate the posterior distributions of the model parameters. Model convergence was assessed with the potential scale reduction statistic $\hat{R}$ (< 1.1 for all parameters), and with visual inspection of the time-series plots of the MCMC samples. To assess a model's goodness of fit, the observed data was visually compared to simulated data generated from the model's posterior predictive distribution (Supplementary Materials).

The ex-Gaussian race model of the stop signal task was fit using the Dynamic Models of Choice (DMC) toolbox version `MBN2019` (Heathcote et al., 2019), implemented in R, version 3.6.1 (R Core Team, 2016). The model ran with 33 chains (i.e., three times the number of parameters), using an automated procedure to continue sampling until convergence was reached (`h.run.unstuck.dmc` and `h.run.converge.dmc` functions in the DMC toolbox). After this, an additional 500 iterations for each chain were obtained to create a final posterior distribution of each parameter, to be used for statistical analyses.

The DDM models were fit using the HDDM toolbox, version 0.8.0 (Wiecki et al., 2013), implemented in Python 3.8.3. Each model ran with 5 chains, with thinning by a factor of 5 to reduce autocorrelations. We obtained 10,000 samples per model and discarded the first 5,000 samples as burn-in, to minimise the effect of initial values on posterior inference.

Statistical inference

Hypothesis testing and statistical inference were performed by comparing the posterior distributions of the patient and control (group node distribution) for each of the parameters of interest. In brief, posterior distributions for each comparison were derived by subtracting the set of MCMC samples of patient and controls. That is, for a given parameter, the difference between the patient and the control group was computed for each MCMC sample, thereby yielding a posterior distribution of the difference. For each comparison, we computed the probability of this difference

distribution being different from zero (no effect) (Makowski et al., 2019), either greater than or smaller than zero (whichever has the highest probability). We report this as the probability of an effect for each comparison, in line with previous research using our modelling approach (Herz et al., 2016). No part of the study procedures was pre-registered prior to the research being conducted.

RESULTS

Model-free behaviour

Basic performance in the task is summarised in Table 1 and in Figures 3A and 3C. The results show that patient accuracy and error rates were similar to the control group. Looking at the raw Go trials, the patient was on average 190 ms faster than controls (patient: M = 470 ms, SD = 133 ms; controls: M = 661 ms, SD = 205 ms). On Stop trials, the tracking algorithm that adapted the SSDs converged well for both patient and controls, reaching a proportion of 51.6% successful stop trials for the patient and a mean of 57.8% (SD = 12.4%) successful stop trials for controls in the final half of the experimental runs ('final stop accuracy'). By contrast, the patient required a stop signal delay that was considerably shorter than controls on average (260 ms vs. 427 ms). We next fit an ex-Gaussian race model to patient and control behaviour in the task, to estimate and formally compare their SSRT and Go RT.

Table 1. Summary of raw measures in the Stop No-Go task.

	Control group mean (SD)	Patient
Go RT (ms)	661.10 (148.0)	469.97
Go overall accuracy (%)	97.31 (4.27)	94.83
Go omission error (%)	1.53 (3.33)	1.48
Go choice error (%)	1.15 (2.25)	3.69
No-Go commission error (%)	1.35 (3.15)	0
Final stop accuracy (%)	57.8 (12.4)	51.6
Mean stop signal delay (ms)	427.73 (106.59)	260.17

Ex-Gaussian model of SSRT and Go RT

The patient had a significantly higher SSRT than controls (Fig. 3B; *probability* = 96.81%), as the posterior of the patient's SSRT (median = 203.52 ms, 95% QI = 170.05-235.40 ms) was distributed across higher values than the posterior of the control group SSRT (median = 165.00 ms, 95% QI = 139.38-188.74 ms). In contrast, the patient's model-derived Go RT (median = 475.79 ms, 95% QI = 463.22-489.56 ms) was significantly lower than the control group mean Go RT (median = 643.63 ms, 95% QI = 587.13-686.22 ms), with no overlap between them (Fig. 3D; *probability* = 100%). Together, these results suggest that although the basic performance of the patient in the task was comparable to controls, he had a deficit in the SSRT, such that he required more time in order to achieve successful stopping in the task. Furthermore, the patient's Go responses in the task were significantly faster than controls. We next examined whether these changes could be explained by changes in the decision threshold, first by fitting a DDM to reaction times in stop trials in which participants failed to inhibit their response.

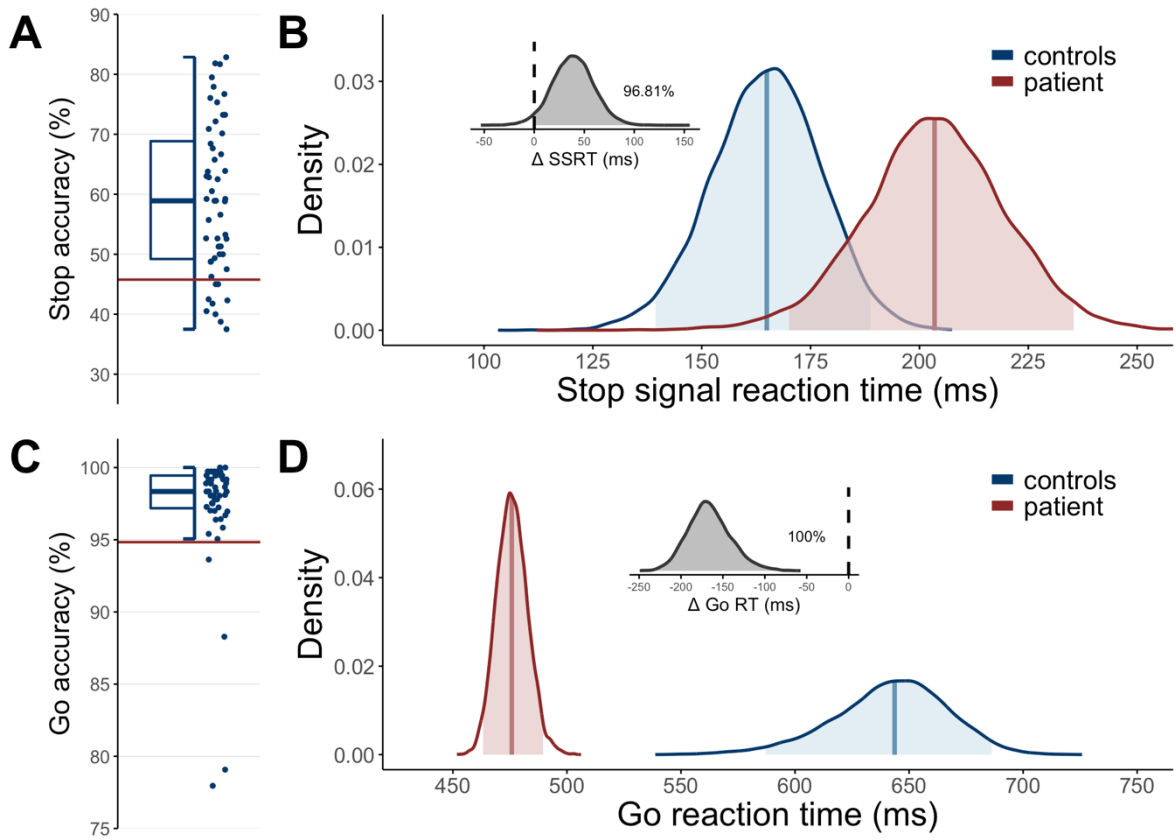

Figure 3. Ex-Gaussian model derived SSRT and Go RT. A) Standard box plot showing the distribution of stop accuracy (probability of successfully stopped responses) in controls (blue box plot and data points) and patient (red line). This shows that across all trials, the algorithm was successful at keeping stop accuracy just above 50%. B) Model derived distributions of the stop signal reaction time (SSRT) parameter for controls (blue) and patient (red), with the distribution of parameter difference (grey) on top. The probability for a group difference in SSRT being different from zero was 96.81%. C) Same as (A) but for Go accuracy, which was the proportion of Go trials in which a response matched the displayed stimulus (right versus left arrow). D) Same as (B) but for the distributions of model derived Go reaction times. The probability for a group difference in Go reacting time being different from zero was 100%.

Drift diffusion modelling of responses

The patient threshold parameter ‘a’ (median = 2.00, 95% QI = 1.27-3.37) was significantly lower than controls (median = 3.59, 95% QI = 3.13-4.24; Fig. 4A;

317 *probability* = 98.62%). In contrast, there were no differences between the patient and
318 controls in the posterior estimates of both drift rate 'v' (Fig. 4B; *probability* = 55.72%;
319 patient: median = 4.64, 95% QI = 3.02-6.44; controls: median = 4.52, 95% QI = 4.21-
320 4.87) and non-decision time 't' (Fig. 4C; *probability* = 73.9%; patient: median = 197.66
321 ms, 95% QI = 123.47-239.19 ms; controls: median = 174.42 ms, 95% QI = 133.74-
322 203.63 ms). These results suggest that the patient required less evidence in order to
323 decide whether to initiate an action (Fig. 4D) due to an abnormally reduced decision
324 threshold.
325
326 This deficit in threshold was for the decision of *whether* to respond. However, it is not
327 clear whether the patient also demonstrated such a deficit in threshold for the decision
328 of *which* action to choose, as suggested by previous neuroimaging research of the
329 pre-SMA (Cavanagh et al., 2011; Mulder et al., 2014; Tosun et al., 2017). Such a
330 deficit would also explain why the patient had significantly faster responses in Go trials
331 (Figure 3D). To test this, we fit a DDM to the RTs and choice data in Go trials. We
332 note, however, that there only a few "incorrect" responses in terms of choice response
333 in the task (see Table 1), which is likely to influence the precision and robustness of
334 parameter estimates.
335

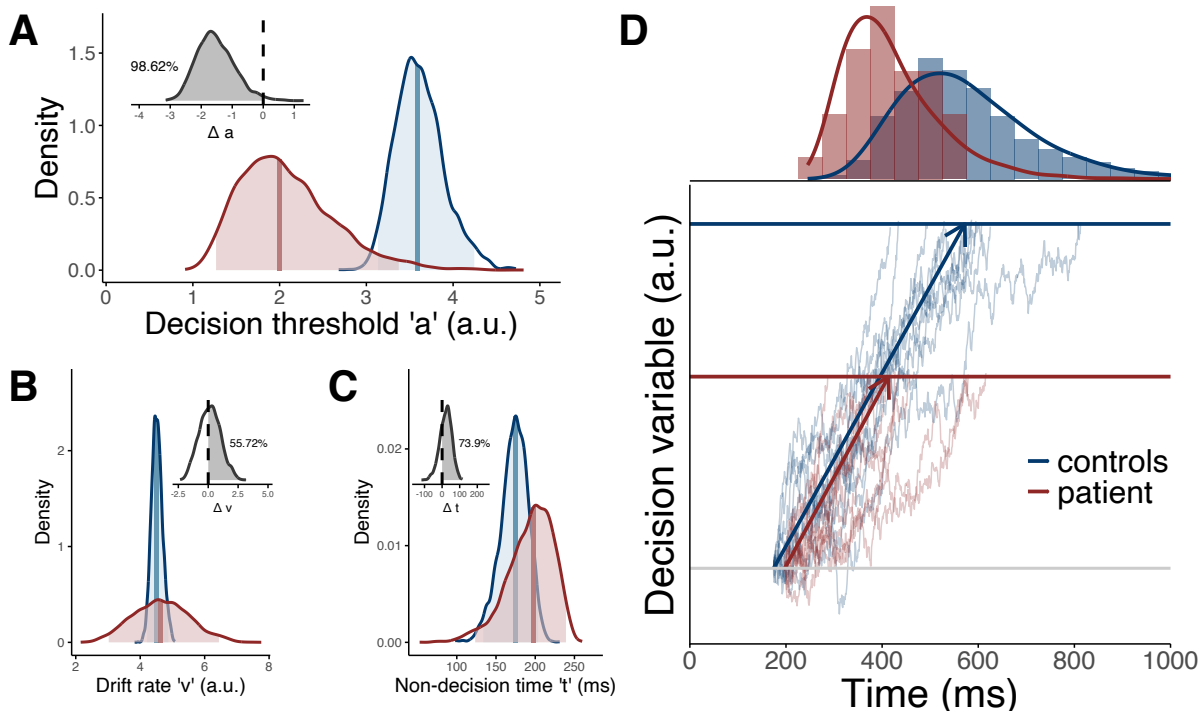

Figure 4. Drift diffusion model parameters for failed Stop trials. Drift diffusion model derived posterior estimates of the decision threshold 'a' (A), drift rate 'v' (B) and non-decision time 't' (C) parameters, for both controls (blue) and patient (red), for the decision to respond in failed Stop trials. Group difference distribution is displayed on top for each of the parameters, with only difference in 'a' being significantly different from zero indicating a significant group difference. D) Simulation of the drift diffusion process for the decision of whether to Stop in failed inhibition trials, based on the control (blue) and patient (red) parameters from A-C. Ten trials were simulated for illustration. Raw (histograms) and fitted (lines) data are plotted on top.

In the context of deciding which button to press, the patient again had a significantly lower threshold (Fig. 5A; *probability* = 100%), with the patient posterior (median = 1.11, 95% QI = 0.95-1.31) distributed across lower values compared to controls (median = 2.00, 95% QI = 1.92-2.13). There was no difference between the patient and controls in the drift rate 'v' (Fig. 5B; *probability* = 89%; patient: median = 3.12, 95% QI = 2.71-3.56; controls: median = 2.86, 95% QI = 2.79-2.93). Lastly, there was no difference

between the patient and controls in non-decision time ‘t’ (Fig. 5C, *probability* = 65.04%; patient: median = 305.56 ms, 95% QI = 275.03-332.49 ms; controls: median = 311.06 ms, 95% QI = 297.04-322.08 ms). The abnormality in decision threshold for action choice in the patient is consistent with previous studies showing the involvement of pre-SMA in modulating choice decision threshold (Cavanagh et al., 2011; Mulder et al., 2014; Tosun et al., 2017).

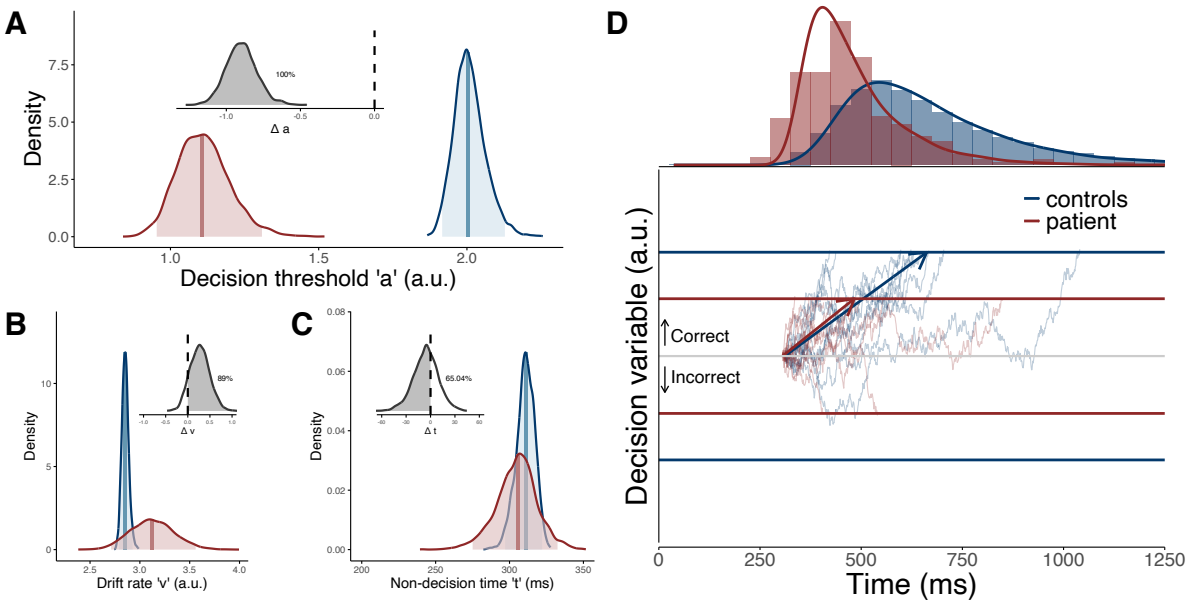

Figure 5. Drift diffusion model parameters for choice accuracy in Go trials. Drift diffusion model derived posterior estimates of the decision threshold ‘a’ (A), drift rate ‘v’ (B) and non-decision time ‘t’ (C) parameters, for both controls (blue) and patient (red), for the decision which button to press in Go trials. Group difference distribution is displayed on top for each of the parameters, with ‘a’ and ‘t’ being significantly different from zero indicating a significant group difference. D) Simulation of the drift diffusion process for the decision of which button to press in the Go trials, based on the control (blue) and patient (red) parameters from A-C. Ten trials were simulated for illustration.

DISCUSSION

The main result of this study is that a focal lesion to the pre-SMA lengthened the time required to stop an action due to an abnormally low response threshold. This was accompanied by a significant increase in response speed due to a similarly reduced threshold for deciding which action to choose. The pre-SMA is known as a key hub for voluntary (Brass & Haggard, 2008) as well as involuntary action (Flamez et al., 2021; Herz et al., 2015; Wolpe et al., 2014). Our results show that dynamic threshold modulation may be a general mechanism by which the pre-SMA exerts its control over actions.

Focal deficits in action threshold setting

Our patient displayed a selective pattern of deficits: lengthened SSRT, with faster Go RT, which were explained by altered thresholds for responding and choosing. This suggests the patient was in fact faster than controls in the tasks, but which rendered him more prone to commission errors in Stop trials – that is, performing an action when asked to withhold. Importantly, the patient made not a single No-Go commission error, indicating a specific difficulty with stopping, rather than a broader multidimensional motor inhibition impairment also encompassing the prevention of prepotent action that is typified by No-Go trials (Chambers et al., 2009; Swick et al., 2011).

The reason why the patient encountered difficulty in stopping is because there is insufficient dynamic shaping of response threshold, such that the response threshold is not dynamically increased in the context of a possible stop cue. Consistent with

previous research into the role of the pre-SMA in decision making for voluntary action (Cavanagh et al., 2011; Mulder et al., 2014; Tosun et al., 2017), we found that the patient showed a similar deficit in threshold setting in the context of deciding which button to choose. Taken together, these results suggest the pre-SMA exert its control over voluntary action by modulating decision thresholds. Such a mechanism may allow the pre-SMA to exert its control over *whether* to perform an action, *when* to perform it and *which* action to perform (Zapparoli et al., 2017).

We note that our study reports the results from one specific case study, rather than a cohort of patients. We further note that the surgical resection was the result of meningioma which is a slow-growing tumour, and plasticity-related brain changes may have influenced his behaviour. The very focal nature of our patient's lesion may arguably have higher validity than a larger cohort of patients with less focal lesions or only limited overlap (Floden & Stuss, 2006). Nevertheless, the obvious extension to this study is to broaden the sample size, while retaining specificity over the anatomical location of the damage. Moreover, the fact that the patient responded more quickly in Go trials may suggest an alternative but related explanation, whereby the patient was unable to choose the appropriate response strategy itself, rather than unable to stop efficiently. Previous studies have indeed shown that response strategies, such as the speed-accuracy trade-off, can affect the response thresholds, for example by increasing response thresholds when accuracy is emphasised (Bogacz et al., 2010; Mansfield et al., 2011). Interestingly, these effects can be experimentally manipulated through instructions, and follow-up research could investigate whether pre-SMA

impairment in decision thresholds can be recoverable by instructing an appropriate response strategy.

Modulation of response threshold by the pre-SMA and its brain interactions

Previous research has suggested that the pre-SMA determines the appropriate threshold when choosing an action, for example to control a speed-accuracy trade-off (Bogacz et al., 2010; Cavanagh et al., 2011; Forstmann et al., 2008; Mulder et al., 2014). In the context of stopping, normal response threshold setting would allow an individual to dynamically shape their behaviour, such that increased response threshold would enable a more cautious strategy of waiting for more evidence to accumulate before responding. By contrast, lower response thresholds would allow for fast responses at the expense of erroneous action initiation (Bogacz et al., 2010).

The pre-SMA exerts its inhibition of unwanted action through its connections with widespread cortical and subcortical brain circuits (Wolpe et al., 2014). Functional (Mansfield et al., 2011) and structural (Forstmann et al., 2012) MRI studies, as well as an interventional stimulation study (Cavanagh et al., 2011), have all pointed to a critical role of the pre-SMA interactions with the striatum in inhibitory control. For example, diffusion MRI-based tractography studies have shown correlations between white matter connections of pre-SMA and striatum with SSRTs in healthy individuals (Forstmann et al., 2012; Rae et al., 2015) and response choice thresholds in older adults (Forstmann et al., 2011). Our findings are consistent with the suggestion that

the pre-SMA exerts inhibition by biasing the striatum to reduce response threshold under more liberal response policy (Cavanagh et al., 2011; Mansfield et al., 2011).

To halt motor activity via the STN, the pre-SMA works in concert with the right inferior frontal gyrus (rIFG) (Aron et al., 2016). A functional connectivity study has shown that the rIFG augments excitatory projections from pre-SMA to STN, thereby amplifying the activation of the STN to “brake” a voluntary action (Rae et al., 2015). A next step would be to extend our approach to also study patients with circumscribed damage to the rIFG. For example, it has been proposed that the rIFG may amplify connectivity in a widely distributed cortical-subcortical network (Aron et al., 2004) to accelerate the evidence accumulation or drift rate (Mulder et al., 2014; White et al., 2014). Testing a patient with rIFG lesion would enable us to examine whether individual differences in the strength of rIFG-STN connectivity during stopping correlates with drift rate. Such a mechanistic dissociation would provide further evidence for a specific role of the rIFG in hastening the implementation of a fast, global, abortive stop process via the STN (Aron et al., 2016; Wessel & Aron, 2013).

The pre-SMA in disorders of voluntary action

The pre-SMA and its connections in a fronto-basal ganglia network are impaired in a number of psychiatric and neurodegenerative conditions. For example, in obsessive-compulsive disorder, abnormally high activity of the pre-SMA (Yücel et al., 2007) accounts for abnormal inhibitory control in patients (de Wit et al., 2012), which is related to patient deficits in the modulation of response thresholds (Banca et al., 2015).

Moreover, patients with the neurodegenerative corticobasal syndrome show a structural impairment in the pre-SMA that correlate with the severity of deficits in voluntary action, such as alien limb (Wolpe et al., 2014). Pre-SMA damage and inability to dynamically adjust response thresholds may lead to the observed disinhibition of action affordance leading to alien limb (McBride et al., 2013). The combination of imaging with models of latent cognitive variables in patient groups could give more concrete insights as to the neurophysiological mechanisms that underlie pathological behaviours. For the estimation of model parameters, Bayesian hierarchical modelling allows robust group-level estimates even in the face of smaller datasets (Ratcliff & Childers, 2015). Such a combined approach will inform future interventional studies to improve clinical outcome in patients.

Conclusions

Damage to the pre-SMA impairs action inhibition by altering response thresholds. A similar deficit was observed for the decision of which action to choose, suggesting that threshold modulation can be a general mechanism by which the pre-SMA exerts its control over voluntary action. Our study illustrates that Bayesian hierarchical model estimation can be used for specific hypothesis testing in single case studies.

DATA & CODE AVAILABILITY

The patient data as well as the analysis and figure plotting code are available on [link to be inserted upon publication]. Control data are available upon signing a data sharing request form on http://www.mrc-cbu.cam.ac.uk/datasets/camcan.

DECLARATION OF INTEREST

The authors declare no conflicts of interest.

ACKNOWLEDGEMENTS

We are grateful to the Cambridge Centre for Ageing and Neuroscience for sharing the data acquired in healthy controls. This work was supported by the James S. McDonnell Foundation 21st Century Science Initiative (Scholar Award to JBR in Understanding Human Cognition) and the Wellcome Trust (103838). NW is funded by a National Institute for Health Research (NIHR), Academic Clinical Fellowship (ACF-2019-14-013). JBR is supported by the Medical Research Council intramural programme (SUAG/051 G101400). FHH was supported by a Cambridge Trust Vice-Chancellor's Award and Fitzwilliam College Scholarship. The views expressed are those of the authors and not necessarily those of the NHS, the NIHR or the Department of Health and Social Care.

REFERENCES

Aron, A. R., Herz, D. M., Brown, P., Forstmann, B. U., & Zaghloul, K. (2016). Frontosubthalamic Circuits for Control of Action and Cognition. *The Journal of Neuroscience*, *36*(45), 11489–11495. https://doi.org/10.1523/JNEUROSCI.2348-16.2016

Aron, A. R., Robbins, T. W., & Poldrack, R. A. (2004). Inhibition and the right inferior frontal cortex. *Trends in Cognitive Sciences*, *8*(4), 170–177. https://doi.org/10.1016/j.tics.2004.02.010

Banca, P., Vestergaard, M. D., Rankov, V., Baek, K., Mitchell, S., Lapa, T., Castelo-Branco, M., & Voon, V. (2015). Evidence Accumulation in Obsessive-Compulsive Disorder: The Role of Uncertainty and Monetary Reward on Perceptual Decision-Making Thresholds. *Neuropsychopharmacology*, *40*(5), 1192–1202. https://doi.org/10.1038/npp.2014.303

Band, G. P. H., van der Molen, M. W., & Logan, G. D. (2003). Horse-race model simulations of the stop-signal procedure. *Acta Psychologica*, *112*(2), 105–142. https://doi.org/10.1016/S0001-6918(02)00079-3

Bogacz, R., Wagenmakers, E.-J., Forstmann, B. U., & Nieuwenhuis, S. (2010). The neural basis of the speed–accuracy tradeoff. *Trends in Neurosciences*, *33*(1), 10–16. https://doi.org/10.1016/j.tins.2009.09.002

Brass, M., & Haggard, P. (2008). The What, When, Whether Model of Intentional Action. *The Neuroscientist*, *14*(4), 319–325. https://doi.org/10.1177/1073858408317417

Cavanagh, J. F., Wiecki, T. V., Cohen, M. X., Figueroa, C. M., Samanta, J., Sherman, S. J., & Frank, M. J. (2011). Subthalamic nucleus stimulation reverses mediofrontal influence

over decision threshold. *Nature Neuroscience*, *14*(11), 1462–1467. https://doi.org/10.1038/nn.2925

Chambers, C. D., Garavan, H., & Bellgrove, M. A. (2009). Insights into the neural basis of response inhibition from cognitive and clinical neuroscience. *Neuroscience & Biobehavioral Reviews*, *33*(5), 631–646. https://doi.org/10.1016/j.neubiorev.2008.08.016

Chen, C., Muggleton, N., Tzeng, O., Hung, D., & Juan, C. (2009). Control of prepotent responses by the superior medial frontal cortex. *NeuroImage*, *44*(2), 537–545. https://doi.org/10.1016/j.neuroimage.2008.09.005

Daw, N. (2011). Trial-by-trial data analysis using computational models. In *Decision making, affect, and learning: Attention and performance XXIII* (Vol. 23, pp. 12–17). Oxford University Press.

de Wit, S. J., de Vries, F. E., van der Werf, Y. D., Cath, D. C., Heslenfeld, D. J., Veltman, E. M., van Balkom, A. J. L. M., Veltman, D. J., & van den Heuvel, O. A. (2012). Presupplementary Motor Area Hyperactivity During Response Inhibition: A Candidate Endophenotype of Obsessive-Compulsive Disorder. *American Journal of Psychiatry*, *169*(10), 1100–1108. https://doi.org/10.1176/appi.ajp.2012.12010073

Dickstein, S. G., Bannon, K., Xavier Castellanos, F., & Milham, M. P. (2006). The neural correlates of attention deficit hyperactivity disorder: An ALE meta-analysis. *Journal of Child Psychology and Psychiatry*, *47*(10), 1051–1062. https://doi.org/10.1111/j.1469-7610.2006.01671.x

Farrell, S., & Lewandowsky, S. (2018). Chapter 9—Multilevel or Hierarchical Modeling. In *Computational Modeling of Cognition and Behavior:* (1st ed.). Cambridge University Press. https://doi.org/10.1017/CBO9781316272503

Flamez, A., Wu, G.-R., Wiels, W., Van Schuerbeek, P., De Mey, J., De Keyser, J., & Baeken, C. (2021). Opposite effects of one session of 1 Hz rTMS on functional connectivity between pre-supplementary motor area and putamen depending on the dyskinesia state in Parkinson's disease. *Clinical Neurophysiology: Official Journal of the International Federation of Clinical Neurophysiology*, *132*(4), 851–856. https://doi.org/10.1016/j.clinph.2020.12.024

Floden, D., & Stuss, D. T. (2006). Inhibitory Control is Slowed in Patients with Right Superior Medial Frontal Damage. *Journal of Cognitive Neuroscience*, *18*(11), 1843–1849. https://doi.org/10.1162/jocn.2006.18.11.1843

Folstein, M. F., Folstein, S. E., & McHugh, P. R. (1975). "Mini-mental state". A practical method for grading the cognitive state of patients for the clinician. *Journal of Psychiatric Research*, *12*(3), 189–198.

Forstmann, B. U., Dutilh, G., Brown, S., Neumann, J., von Cramon, D. Y., Ridderinkhof, K. R., & Wagenmakers, E.-J. (2008). Striatum and pre-SMA facilitate decision-making under time pressure. *Proceedings of the National Academy of Sciences*, *105*(45), 17538–17542. https://doi.org/10.1073/pnas.0805903105

Forstmann, B. U., Keuken, M. C., Jahfari, S., Bazin, P.-L., Neumann, J., Schäfer, A., Anwander, A., & Turner, R. (2012). Cortico-subthalamic white matter tract strength predicts interindividual efficacy in stopping a motor response. *NeuroImage*, *60*(1), 370–375. https://doi.org/10.1016/j.neuroimage.2011.12.044

Forstmann, B. U., Tittgemeyer, M., Wagenmakers, E.-J., Derrfuss, J., Imperati, D., & Brown, S. (2011). The speed-accuracy tradeoff in the elderly brain: A structural model-based approach. *The Journal of Neuroscience*, *31*(47), 17242–17249. https://doi.org/10.1523/JNEUROSCI.0309-11.2011

Fried, I., Katz, A., McCarthy, G., Sass, K. J., Williamson, P., Spencer, S. S., & Spencer, D. D. (1991). Functional organization of human supplementary motor cortex studied by electrical stimulation. *The Journal of Neuroscience*, *11*(11), 3656–3666.

Gelman, A., Carlin, J. B., Stern, H. S., Dunson, D. B., Vehtari, A., & Rubin, D. B. (2014). *Bayesian data analysis* (Third edition). CRC Press, Taylor and Francis Group.

Heathcote, A., Lin, Y.-S., Reynolds, A., Strickland, L., Gretton, M., & Matzke, D. (2019). Dynamic models of choice. *Behavior Research Methods*, *51*(2), 961–985. https://doi.org/10.3758/s13428-018-1067-y

Heathcote, A., Popiel, S. J., & Mewhort, D. J. (1991). Analysis of response time distributions: An example using the Stroop task. *Psychological Bulletin*, *109*(2), 340–347. https://doi.org/10.1037/0033-2909.109.2.340

Herz, D. M., Haagensen, B. N., Christensen, M. S., Madsen, K. H., Rowe, J. B., Løkkegaard, A., & Siebner, H. R. (2015). Abnormal dopaminergic modulation of striato-cortical networks underlies levodopa-induced dyskinesias in humans. *Brain*, *138*(6), 1658–1666. https://doi.org/10.1093/brain/awv096

Herz, D. M., Zavala, B. A., Bogacz, R., & Brown, P. (2016). Neural Correlates of Decision Thresholds in the Human Subthalamic Nucleus. *Current Biology*, *26*(7), 916–920. https://doi.org/10.1016/j.cub.2016.01.051

Limongi, R., Bohaterewicz, B., Nowicka, M., Plewka, A., & Friston, K. J. (2018). Knowing when to stop: Aberrant precision and evidence accumulation in schizophrenia. *Schizophrenia Research*, *197*, 386–391. https://doi.org/10.1016/j.schres.2017.12.018

Logan, G. D., & Cowan, W. B. (1984). On the ability to inhibit thought and action: A theory of an act of control. *Psychological Review*, *91*(3), 295–327. https://doi.org/10.1037/0033-295X.91.3.295

Makowski, D., Ben-Shachar, M. S., Chen, S. H. A., & Lüdecke, D. (2019). Indices of Effect Existence and Significance in the Bayesian Framework. *Frontiers in Psychology*, *10*. https://doi.org/10.3389/fpsyg.2019.02767

Mansfield, E. L., Karayanidis, F., Jamadar, S., Heathcote, A., & Forstmann, B. U. (2011). Adjustments of Response Threshold during Task Switching: A Model-Based Functional Magnetic Resonance Imaging Study. *Journal of Neuroscience*, *31*(41), 14688–14692. https://doi.org/10.1523/JNEUROSCI.2390-11.2011

Matzke, D., Curley, S., Gong, C. Q., & Heathcote, A. (2019). Inhibiting responses to difficult choices. *Journal of Experimental Psychology: General*, *148*(1), 124–142. https://doi.org/10.1037/xge0000525

Matzke, D., Dolan, C. V., Logan, G. D., Brown, S. D., & Wagenmakers, E.-J. (2013). Bayesian parametric estimation of stop-signal reaction time distributions. *Journal of Experimental Psychology: General*, *142*(4), 1047–1073. https://doi.org/10.1037/a0030543

Matzke, D., Hughes, M., Badcock, J. C., Michie, P., & Heathcote, A. (2017). Failures of cognitive control or attention? The case of stop-signal deficits in schizophrenia.

Attention, Perception, & Psychophysics, *79*(4), 1078–1086. https://doi.org/10.3758/s13414-017-1287-8

Matzke, D., Logan, G. D., & Heathcote, A. (2020). A Cautionary Note on Evidence-Accumulation Models of Response Inhibition in the Stop-Signal Paradigm. *Computational Brain & Behavior*, *3*(3), 269–288. https://doi.org/10.1007/s42113-020-00075-x

Matzke, D., Love, J., & Heathcote, A. (2017). A Bayesian approach for estimating the probability of trigger failures in the stop-signal paradigm. *Behavior Research Methods*, *49*(1), 267–281. https://doi.org/10.3758/s13428-015-0695-8

Matzke, D., & Wagenmakers, E.-J. (2009). Psychological interpretation of the ex-Gaussian and shifted Wald parameters: A diffusion model analysis. *Psychonomic Bulletin & Review*, *16*(5), 798–817. https://doi.org/10.3758/PBR.16.5.798

McBride, J., Sumner, P., Jackson, S. R., Bajaj, N., & Husain, M. (2013). Exaggerated object affordance and absent automatic inhibition in alien hand syndrome. *Cortex*, *49*(8), 2040–2054. https://doi.org/10.1016/j.cortex.2013.01.004

Mulder, M. J., van Maanen, L., & Forstmann, B. U. (2014). Perceptual decision neurosciences—A model-based review. *Neuroscience*, *277*, 872–884. https://doi.org/10.1016/j.neuroscience.2014.07.031

Passamonti, L., Lansdall, C., & Rowe, J. (2018). The neuroanatomical and neurochemical basis of apathy and impulsivity in frontotemporal lobar degeneration. *Current Opinion in Behavioral Sciences*, *22*, 14–20. https://doi.org/10.1016/j.cobeha.2017.12.015

R Core Team, . (2016). *R: A language and environment for statistical computing*. R Foundation for Statistical Computing. http://www.r-project.org/

Rae, C. L., Hughes, L. E., Anderson, M. C., & Rowe, J. B. (2015). The Prefrontal Cortex Achieves Inhibitory Control by Facilitating Subcortical Motor Pathway Connectivity. *The Journal of Neuroscience*, *35*(2), 786–794. https://doi.org/10.1523/JNEUROSCI.3093-13.2015

Rae, C. L., Hughes, L. E., Weaver, C., Anderson, M. C., & Rowe, J. B. (2014). Selection and stopping in voluntary action: A meta-analysis and combined fMRI study. *Neuroimage*, *86*, 381–391.

Ratcliff, R., & Childers, R. (2015). Individual Differences and Fitting Methods for the Two-Choice Diffusion Model of Decision Making. *Decision (Washington, D.C.)*, *2015*, 10.1037/dec0000030.

Ratcliff, R., & McKoon, G. (2008). The Diffusion Decision Model: Theory and Data for Two-Choice Decision Tasks. *Neural Computation*, *20*(4), 873–922. https://doi.org/10.1162/neco.2008.12-06-420

Ratcliff, R., & Tuerlinckx, F. (2002). Estimating parameters of the diffusion model: Approaches to dealing with contaminant reaction times and parameter variability. *Psychonomic Bulletin & Review*, *9*(3), 438–481. https://doi.org/10.3758/BF03196302

Ratcliff, R., & Van Dongen, H. P. A. (2011). Diffusion model for one-choice reaction-time tasks and the cognitive effects of sleep deprivation. *Proceedings of the National Academy of Sciences*, *108*(27), 11285–11290. https://doi.org/10.1073/pnas.1100483108

Sebastian, A., Forstmann, B. U., & Matzke, D. (2018). Towards a model-based cognitive neuroscience of stopping – a neuroimaging perspective. *Neuroscience & Biobehavioral Reviews*, *90*, 130–136. https://doi.org/10.1016/j.neubiorev.2018.04.011

Shafto, M. A., Tyler, L. K., Dixon, M., Taylor, J. R., Rowe, J. B., Cusack, R., Calder, A. J., Marslen-Wilson, W. D., Duncan, J., Dalgleish, T., Henson, R. N., Brayne, C., & Matthews, F. E. (2014). The Cambridge Centre for Ageing and Neuroscience (Cam-CAN) study protocol: A cross-sectional, lifespan, multidisciplinary examination of healthy cognitive ageing. *BMC Neurology*, *14*(1), 204. https://doi.org/10.1186/s12883-014-0204-1

Skippen, P., Matzke, D., Heathcote, A., Fulham, W. R., Michie, P., & Karayanidis, F. (2019). Reliability of triggering inhibitory process is a better predictor of impulsivity than SSRT. *Acta Psychologica*, *192*, 104–117. https://doi.org/10.1016/j.actpsy.2018.10.016

Smith, S. M. (2002). Fast robust automated brain extraction. *Human Brain Mapping*, *17*(3), 143–155. https://doi.org/10.1002/hbm.10062

Swick, D., Ashley, V., & Turken, U. (2011). Are the neural correlates of stopping and not going identical? Quantitative meta-analysis of two response inhibition tasks. *NeuroImage*, *56*(3), 1655–1665. https://doi.org/10.1016/j.neuroimage.2011.02.070

Tosun, T., Berkay, D., Sack, A. T., Çakmak, Y. Ö., & Balcı, F. (2017). Inhibition of Pre–Supplementary Motor Area by Continuous Theta Burst Stimulation Leads to More Cautious Decision-making and More Efficient Sensory Evidence Integration. *Journal of Cognitive Neuroscience*, *29*(8), 1433–1444. https://doi.org/10.1162/jocn_a_01134

Tsvetanov, K. A., Ye, Z., Hughes, L., Samu, D., Treder, M. S., Wolpe, N., Tyler, L. K., Rowe, J. B., & for the Cambridge Centre for Ageing and Neuroscience. (2018). Activity and Connectivity Differences Underlying Inhibitory Control Across the Adult Life Span. *The Journal of Neuroscience*, *38*(36), 7887–7900. https://doi.org/10.1523/JNEUROSCI.2919-17.2018

van Maanen, L., Brown, S. D., Eichele, T., Wagenmakers, E.-J., Ho, T., Serences, J., & Forstmann, B. U. (2011). Neural correlates of trial-to-trial fluctuations in response caution. *Journal of Neuroscience*, *31*(48), 17488–17495. https://doi.org/10.1523/JNEUROSCI.2924-11.2011

Weigard, A., Heathcote, A., Matzke, D., & Huang-Pollock, C. (2019). Cognitive Modeling Suggests That Attentional Failures Drive Longer Stop-Signal Reaction Time Estimates in Attention Deficit/Hyperactivity Disorder. *Clinical Psychological Science*, *7*(4), 856–872. https://doi.org/10.1177/2167702619838466

Wessel, J. R., & Aron, A. R. (2013). Unexpected Events Induce Motor Slowing via a Brain Mechanism for Action-Stopping with Global Suppressive Effects. *Journal of Neuroscience*, *33*(47), 18481–18491. https://doi.org/10.1523/JNEUROSCI.3456-13.2013

White, C. N., Congdon, E., Mumford, J. A., Karlsgodt, K. H., Sabb, F. W., Freimer, N. B., London, E. D., Cannon, T. D., Bilder, R. M., & Poldrack, R. A. (2014). Decomposing Decision Components in the Stop-signal Task: A Model-based Approach to Individual Differences in Inhibitory Control. *Journal of Cognitive Neuroscience*, *26*(8), 1601–1614. https://doi.org/10.1162/jocn_a_00567

Wiecki, T. V., Sofer, I., & Frank, M. J. (2013). HDDM: Hierarchical Bayesian estimation of the Drift-Diffusion Model in Python. *Frontiers in Neuroinformatics*, *7*. https://doi.org/10.3389/fninf.2013.00014

Wolpe, N., Moore, J. W., Rae, C. L., Rittman, T., Altena, E., Haggard, P., & Rowe, J. B. (2014). The medial frontal-prefrontal network for altered awareness and control of action in corticobasal syndrome. *Brain*, *137*(1), 208–220. https://doi.org/10.1093/brain/awt302

Yücel, M., Harrison, B. J., Wood, S. J., Fornito, A., Wellard, R. M., Pujol, J., Clarke, K., Phillips, M. L., Kyrios, M., Velakoulis, D., & Pantelis, C. (2007). Functional and Biochemical Alterations of the Medial Frontal Cortex in Obsessive-Compulsive Disorder. *Archives of General Psychiatry*, *64*(8), 946. https://doi.org/10.1001/archpsyc.64.8.946

Zapparoli, L., Seghezzi, S., & Paulesu, E. (2017). The What, the When, and the Whether of Intentional Action in the Brain: A Meta-Analytical Review. *Frontiers in Human Neuroscience*, *11*. https://doi.org/10.3389/fnhum.2017.00238

SUPPLEMENTARY MATERIALS

Table S1. Priors for the ex-Gaussian race model

Parameter	Group-level prior distributions		
Mean of Gaussian component of matching go process ($\mu_{\text{go-match}}$)	$\mu_{\mu_{\text{go-match}}}$	$\sim$	$\mathcal{N}_+(1.5, 1)$
	$\sigma_{\mu_{\text{go-match}}}$	$\sim$	$\exp(1)$
Mean of Gaussian component of mismatching go process ($\mu_{\text{go-mismatch}}$)	$\mu_{\mu_{\text{go-mismatch}}}$	$\sim$	$\mathcal{N}_+(1.5, 1)$
	$\sigma_{\mu_{\text{go-mismatch}}}$	$\sim$	$\exp(1)$
Mean of Gaussian component of stop process (μ_{stop})	$\mu_{\mu_{\text{stop}}}$	$\sim$	$\mathcal{N}_+(1, 1)$
	$\sigma_{\mu_{\text{stop}}}$	$\sim$	$\exp(1)$
Standard deviation of Gaussian component of matching go process ($\sigma_{\text{go-match}}$)	$\mu_{\sigma_{\text{go-match}}}$	$\sim$	$\mathcal{N}_+(0.2, 1)$
	$\sigma_{\sigma_{\text{go-match}}}$	$\sim$	$\exp(1)$
Standard deviation of Gaussian component of mismatching go process ($\sigma_{\text{go-mismatch}}$)	$\mu_{\sigma_{\text{go-mismatch}}}$	$\sim$	$\mathcal{N}_+(0.2, 1)$
	$\sigma_{\sigma_{\text{go-mismatch}}}$	$\sim$	$\exp(1)$
Standard deviation of Gaussian component of stop process (σ_{stop})	$\mu_{\sigma_{\text{stop}}}$	$\sim$	$\mathcal{N}_+(0.2, 1)$
	$\sigma_{\sigma_{\text{stop}}}$	$\sim$	$\exp(1)$
Mean of exponential component of matching go process ($\tau_{\text{go-match}}$)	$\mu_{\tau_{\text{go-match}}}$	$\sim$	$\mathcal{N}_+(0.2, 1)$
	$\sigma_{\tau_{\text{go-match}}}$	$\sim$	$\exp(1)$
Mean of exponential component of mismatching go process ($\tau_{\text{go-mismatch}}$)	$\mu_{\tau_{\text{go-mismatch}}}$	$\sim$	$\mathcal{N}_+(0.2, 1)$
	$\sigma_{\tau_{\text{go-mismatch}}}$	$\sim$	$\exp(1)$
Mean of exponential component of stop process (τ_{stop})	$\mu_{\tau_{\text{stop}}}$	$\sim$	$\mathcal{N}_+(0.2, 1)$
	$\sigma_{\tau_{\text{stop}}}$	$\sim$	$\exp(1)$
Probit transformed trigger failure probability [$\Phi^{-1}(P_{\text{TF}})$]	$\mu_{\Phi^{-1}(P_{\text{TF}})}$	$\sim$	$\mathcal{N}(\Phi^{-1}(0.1), 1)$
	$\sigma_{\Phi^{-1}(P_{\text{TF}})}$	$\sim$	$\exp(1)$
Probit transformed go failure probability [$\Phi^{-1}(P_{\text{GF}})$]	$\mu_{\Phi^{-1}(P_{\text{GF}})}$	$\sim$	$\mathcal{N}(\Phi^{-1}(0.1), 1)$
	$\sigma_{\Phi^{-1}(P_{\text{GF}})}$	$\sim$	$\exp(1)$

$\mathcal{N}(\mu, \sigma)$ denotes a normal distribution with mean μ and standard deviation σ; $\mathcal{N}_+(\mu, \sigma)$ denotes a positive normal distribution truncated at zero; $\exp(\lambda)$ denotes an exponential distribution with a rate parameter λ; $\Phi^{-1}(p)$ denotes the probit function

(i.e., the inverse cumulative distribution function of the standard normal distribution) evaluated at probability p. All parameters are on the scale of seconds, except for the trigger and go failure probabilities. For the patient non-hierarchical model fit, the priors were identical to the priors on the control group-level.

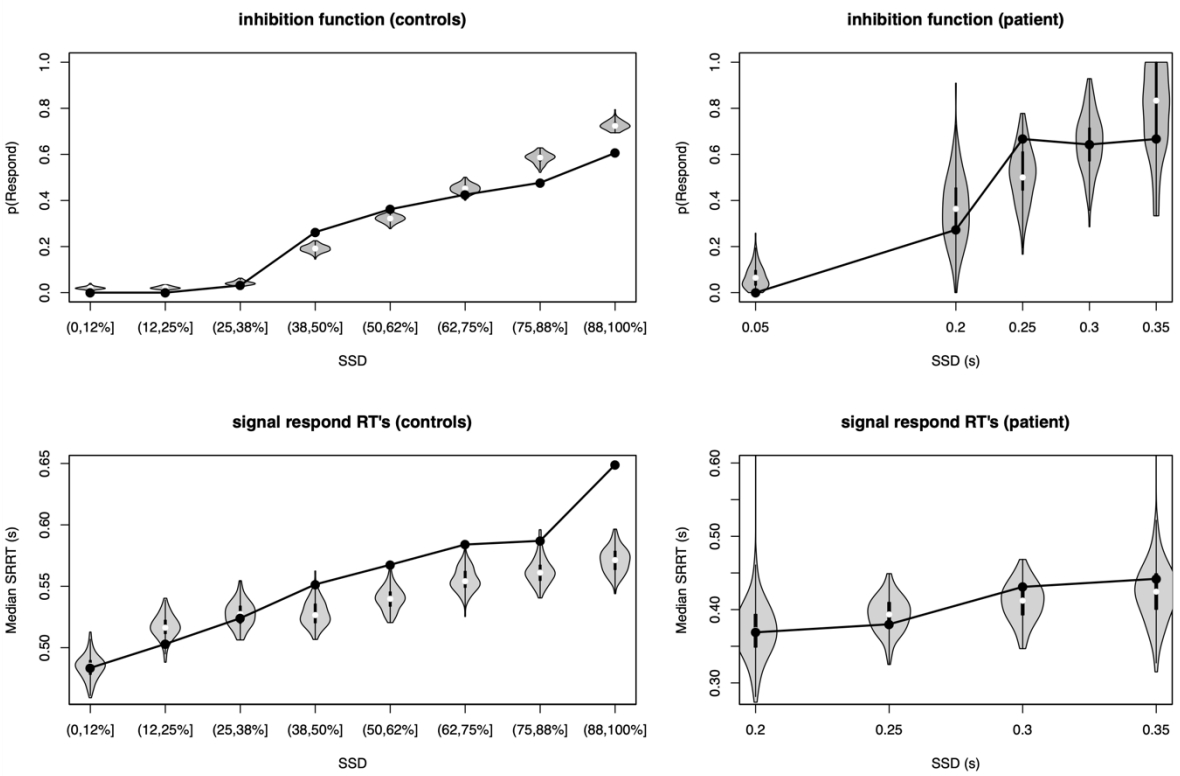

Figure S1. Posterior predictive checks of stopping performance. Inhibition function plots (top row) showing the mean probability of responding as a function of SSD for controls (left column) and patient (right column). The bottom row plots the median RTs of failed stop trials (i.e., signal respond RT) as a function of SSD. For the control group plots, the SSD's have been grouped into percentile bins of approximately equal size. For the patient plots, we excluded SSD bins with less than 5 trials for the inhibition function, and less than 3 trials for the signal respond RTs. Grey violin plots show the posterior predictive distributions. Data shown as black dots and connecting lines.

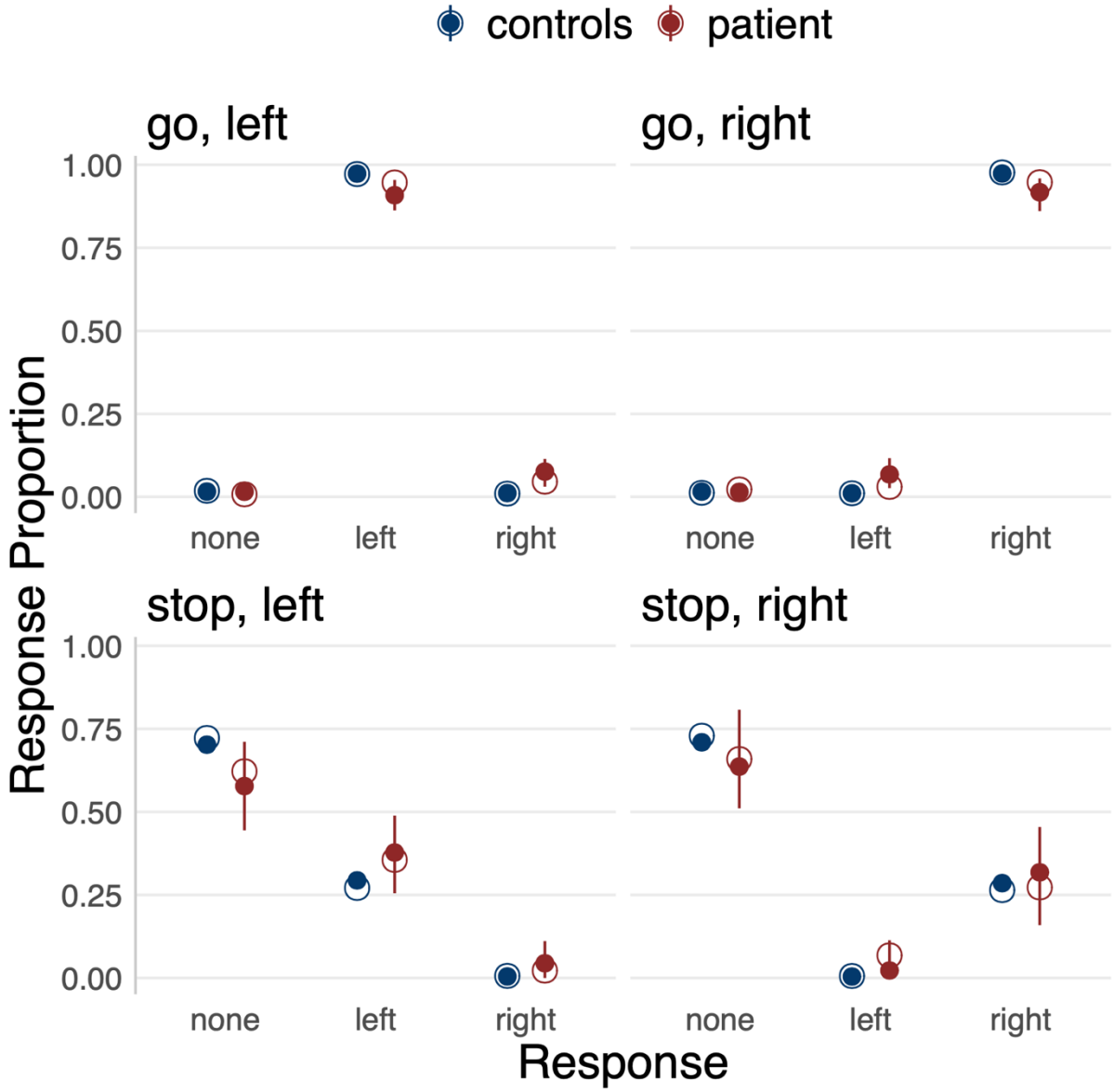

Figure S2. Posterior predictive checks of response proportions. Response proportions for Go (top row) and Stop (bottom row) trials for both controls (blue) and patient (red). Response proportions are shown separately for each stimulus (left versus right arrow) and are plotted as a function of response type (no response; left and right response). Empty dots indicate data (mean). Filled dots ± error bars indicate posterior predictive distributions.

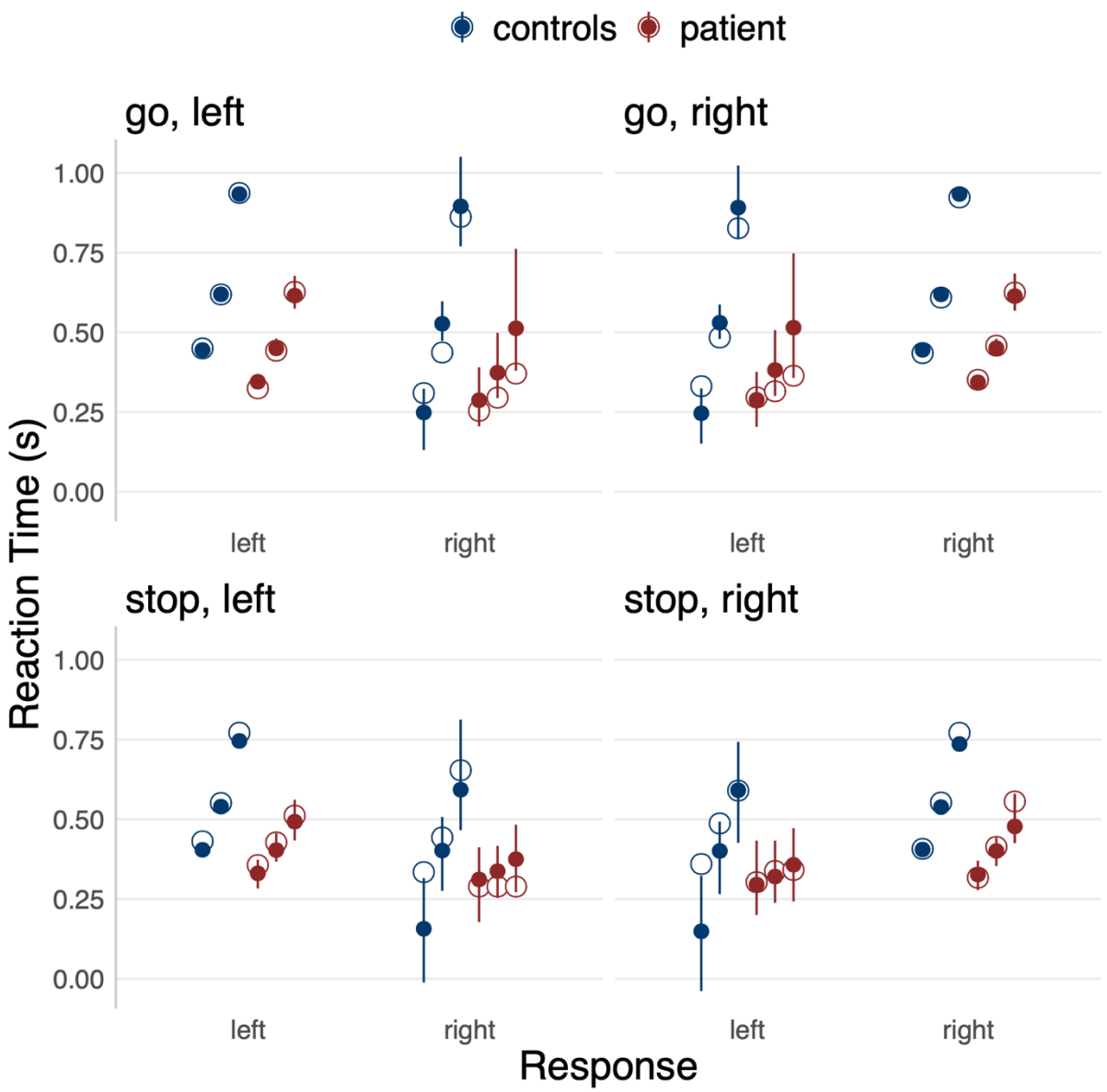

Figure S3. Posterior predictive checks of reaction times. Reaction times for Go (top row) and Stop (bottom row) trials for both controls (blue) and patient (red). Response times are shown separately for each stimulus (left versus right arrow. Empty dots indicate data (mean). Filled dots ± error bars indicate posterior predictive distributions. The three dots indicate the 10th, 50th, and 90th quantiles of the RT distributions.

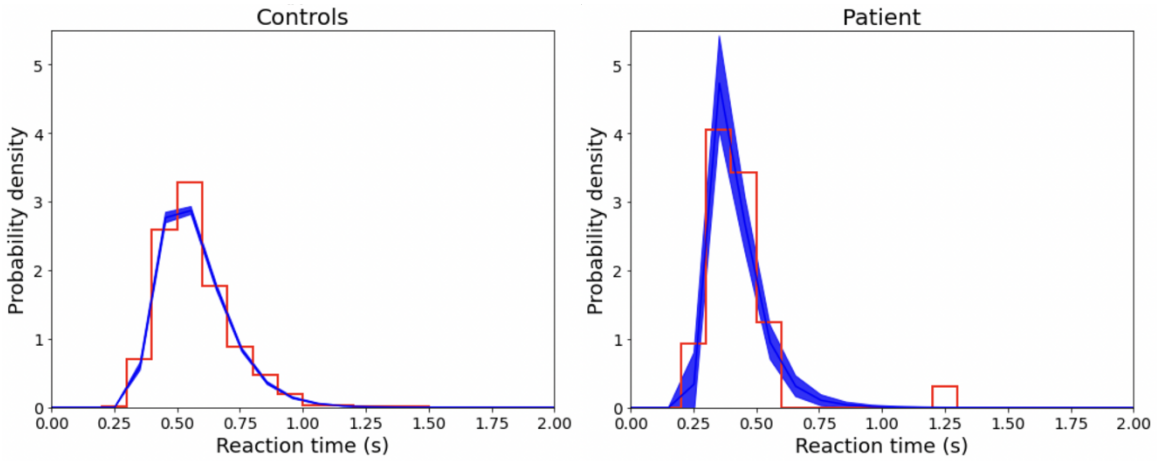

Figure S4. Posterior predictive checks of reaction time distributions for response in failed Stop trials. The plots show the reaction time distributions for controls (left panel) and for the patient (right panel) for unsuccessful Stop trials, in which participants failed to inhibit their response. There were no meaningful differences in deviance information criterion between the model with or without 'st' (-1843.79 versus -1842.31 for controls and -53.17 versus -50.22 for the patient, respectively). The simpler model without 'st' was therefore used when reporting the parameters. Data are shown in red histograms, and model predictions are overlaid in blue, generated by drawing 1000 samples from the posterior parameter estimates.

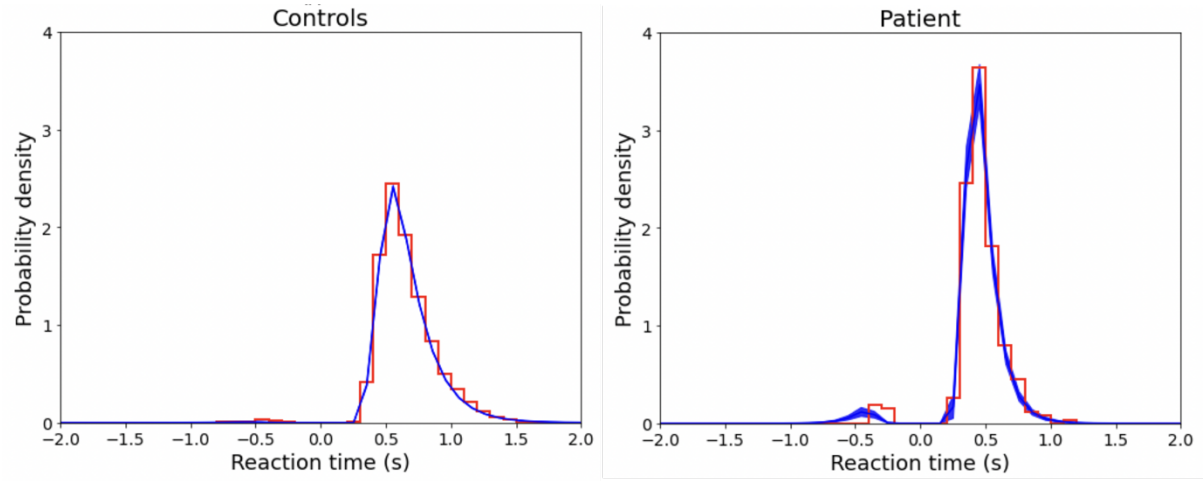

Figure S5. Posterior predictive checks of reaction time distributions for response choice accuracy in Go trials. The plots show the reaction time distributions for controls (left panel) and for the patient (right panel) for Go trials. Correct choices are plotted as positive reaction times and incorrect choices are plotted as negative reaction times. There were meaningful differences in deviance information criterion between the model with and without ‘st’ (-6803.63 versus -6771.10 for controls and -286.16 versus -268.10 for the patient, respectively). The model that included ‘st’ was therefore used when reporting the parameters. Data are shown in red histograms, and model predictions are overlaid in blue, generated by drawing 1000 samples from the posterior parameter estimates.